
DSDR: Dual-Scale Diversity Regularization for Exploration in LLM Reasoning

Zhongwei Wan^{*1} Yun Shen^{*1} Zhihao Dou² Donghao Zhou³ Yu Zhang⁴ Xin Wang¹ Hui Shen⁵
 Jing Xiong⁶ Chaofan Tao⁶ Zixuan Zhong⁷ Peizhou Huang⁵ Mi Zhang¹

Abstract

Reinforcement learning with verifiers (RLVR) is a central paradigm for improving large language model (LLM) reasoning, yet existing methods often suffer from limited exploration. Policies tend to collapse onto a few reasoning patterns and prematurely stop deep exploration, while conventional entropy regularization introduces only local stochasticity and fails to induce meaningful path-level diversity, leading to weak and unstable learning signals in group-based policy optimization. We propose **DSDR**, a *Dual-Scale Diversity Regularization* reinforcement learning framework that decomposes diversity in LLM reasoning into global and coupling components. Globally, DSDR promotes diversity among correct reasoning trajectories to explore distinct solution modes. Locally, it applies a length-invariant, token-level entropy regularization restricted to correct trajectories, preventing entropy collapse within each mode while preserving correctness. The two scales are coupled through a global-to-local allocation mechanism that emphasizes local regularization for more distinctive correct trajectories. We provide theoretical support showing that DSDR preserves optimal correctness under bounded regularization, sustains informative learning signals in group-based optimization, and yields a principled global-to-local coupling rule. Experiments on multiple reasoning benchmarks demonstrate consistent improvements in accuracy and pass@k, highlighting the importance of dual-scale diversity for deep exploration in RLVR. Code is available at [DSDR](#).

1. Introduction

Reinforcement learning with verified reward (RLVR) (Liu et al., 2024; Shao et al., 2024) has recently emerged as a powerful paradigm for enhancing the reasoning capabilities of LLMs. Group-based policy optimization methods, such as GRPO (Guo et al., 2025), further improve training stability by exploiting relative comparisons among sampled solutions, making RLVR practical at scale. By leveraging outcome-based supervision rather than token-level imitation, RLVR has enabled substantial improvements in math and code reasoning, logical inference, and multi-step problem solving, and has become a core component of recent advances in reasoning-oriented LLM training (Comanici et al., 2025; Singh et al., 2025; Yang et al., 2025).

Despite these successes, verified reward-maximizing RL training often exhibits limited deep exploration, even when alternative valid solution paths exist (Liu et al., 2025b; Shen, 2025; Wu et al., 2025; Chen et al., 2025a). This phenomenon is widely observed across RLVR pipelines: while models improve pass@1 accuracy, they often do so by concentrating probability mass on a small set of homogeneous reasoning patterns, leading to a collapse in solution diversity. Consequently, pass@k performance fails to improve and generalization deteriorates, especially when models are evaluated on out-of-domain or more compositional reasoning tasks (Walder & Karkhanis, 2025; Jiang et al., 2025).

A natural response is to encourage diversified exploration during training, yet existing methods remain insufficient. Entropy regularization (Shen, 2025; Chen et al., 2025c; Agarwal et al., 2025), widely used in RL and RLVR, injects token-level stochasticity but mainly induces local randomness and fails to promote distinct reasoning paths. Conversely, recent diversity-driven methods (Zhang et al., 2025; Chen et al., 2025b; Li et al., 2025; Hu et al., 2025) encourage variation among generated solutions, sometimes with quality or correctness constraints. However, these approaches are typically single-scale or weakly coupled across scales: token-level entropy or uncertainty control induces local stochasticity and rarely sustains distinct reasoning trajectories, while trajectory-level diversity alone fails to prevent intra-mode entropy collapse once a few correct templates dominate. Consequently, policies may still prematurely con-

¹The Ohio State University, USA ²Case Western Reserve University, USA ³The Chinese University of Hong Kong, Hong Kong ⁴Macquarie University, Australia ⁵University of Michigan, USA ⁶The University of Hong Kong, Hong Kong ⁷University College London, UK. Correspondence to: Zhongwei Wan <wan.512@osu.edu>, Mi Zhang <mizhang.1@osu.edu>.

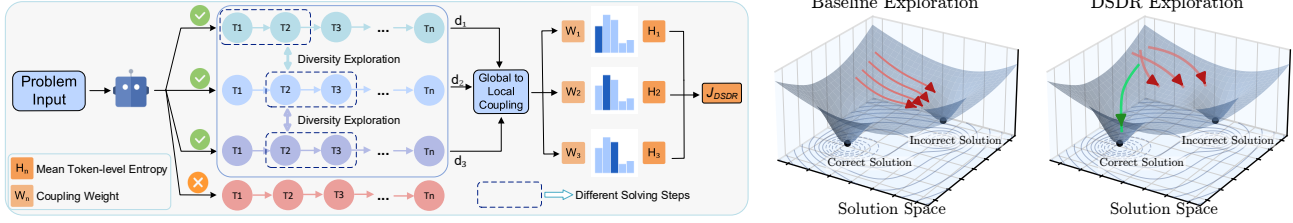


Figure 1. (Left): global-to-local coupling for enhanced exploration during RL training. (Right): baseline exploration collapses to local suboptimal solutions, while DSDR promotes diverse trajectories that escape local optima and reach the correct solution space.

centrate on a small set of correct reasoning modes, and in group-normalized RLVR this concentration weakens within-group preference signals as verifier rewards become nearly constant. The core tension between deep exploration and correctness therefore remains unresolved, requiring exploration to be correctness-aligned and explicitly coordinated across both trajectory- and token-scales.

This motivates a dual-scale formulation of exploration for LLM reasoning. (i) At the global level, exploration requires discovering and maintaining multiple distinct reasoning modes, corresponding to different solution paths. (ii) At the local level, exploration requires preventing premature entropy collapse (Cui et al., 2025; Shen, 2025) within each mode, so that correct trajectories remain robust and expressive rather than brittle or over-confident. Crucially, these two forms of diversity are complementary and can be jointly optimized rather than treated in isolation, since not all correct modes are equally valuable for further exploration, motivating a mechanism that allocates local regularization based on global distinctiveness.

Building on this insight, we propose **DSDR**, a *Dual-Scale Diversity Regularization* framework for RL-based LLM reasoning. DSDR integrates global diversity regularization over correct reasoning trajectories with a length-invariant, token-level entropy term applied exclusively to correct solutions. As illustrated in Figure 1, these two scales are coupled through a global-to-local allocation mechanism, which prioritizes local regularization for more distinctive correct trajectories. Additionally, this coupling prevents exploration from collapsing into narrow, locally suboptimal reasoning templates, instead promoting diverse trajectories that escape local optima and expand the correct solution space. We further provide theoretical support for DSDR, showing that bounded positive-only local entropy preserves optimal correctness, while correct-only global shaping prevents signal degeneracy in group-normalized optimization. We also justify the global-to-local softmax coupling from a principled objective view, explaining why dual-scale diversity strengthens learning signals. Extensive experiments across multiple reasoning benchmarks demonstrate that DSDR consistently improves accuracy, pass@k performance, and training sta-

bility, highlighting the importance of principled dual-scale diversity for deep exploration in RLVR. Our main contributions are summarized as follows:

- We introduce a dual-scale perspective on exploration in LLM reasoning, explicitly distinguishing global (inter-mode) and local (intra-mode) diversity and clarifying their complementary roles in RLVR.
- We propose DSDR, a correctness-aligned dual-scale diversity regularization framework that couples global diversity with positive-only, length-invariant local entropy through a global-to-local allocation mechanism.
- We provide theoretical support for correctness preservation and signal preservation in group-normalized RLVR, together with a principled interpretation of the global-to-local coupling, validated by consistent empirical gains.

2. Related Work

RLVR and Exploration in LLMs. Reinforcement learning with verifiable rewards (RLVR) has become a prominent approach for improving LLM reasoning (Cobbe et al., 2021; Singh et al., 2025; Guo et al., 2025). While this training can elicit emergent reasoning behaviors such as verification and self-reflection (Gandhi et al., 2025; Wan et al., 2025), it often suffers from limited exploration, where policies converge early to a narrow set of reasoning patterns, resulting in performance plateaus. To mitigate this issue, prior work has explored a range of exploration-enhancing strategies, including increasing policy stochasticity through entropy regularization or temperature adjustment (Hou et al., 2025), modifying optimization objectives via relaxed clipping or pass@k-based rewards (Yu et al., 2025; Chen et al., 2025c), and intervening in rollout dynamics to encourage mode switching, such as the sample-then-forget mechanism (Chen et al., 2025a). While these approaches improve exploration from different angles, they either rely on unstructured randomness, objective-level relaxation, or rollout-level interventions, and do not explicitly model how exploration should be coordinated across different scales of reasoning. Instead, our work attempt to address exploration

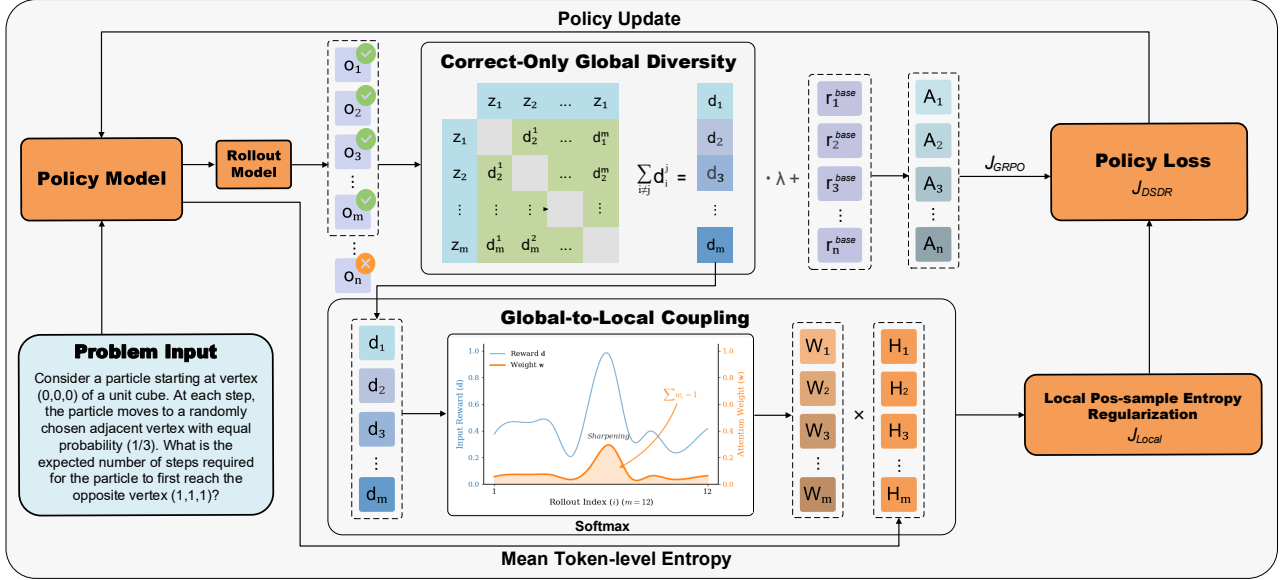


Figure 2. DSDR training pipeline for dual-scale exploration in RL. Correct-only global diversity promotes exploration across solution modes, while a global-to-local coupling mechanism allocates length-invariant local entropy regularization to distinctive correct trajectories. Both signals are integrated into policy updates to enable deep exploration without sacrificing correctness.

limitations by structuring diversity directly within policy optimization across global-to-local scales, enabling deep exploration without modifying rollout procedures.

Diversity and Entropy Control for LLM Reasoning. Recent studies have explored promoting diversity in LLM reasoning by manipulating uncertainty at different levels of the policy. Token-level methods selectively encourage stochastic actions through entropy bonuses, clipping, or KL constraints (Cui et al., 2025; Liu et al., 2025a; Yu et al., 2025; Agarwal et al., 2025; Shen, 2025; Yao et al., 2025), which can alleviate premature collapse but primarily operate at a local action level. While effective in increasing short-term randomness, these methods do not explicitly encourage diversity across complete reasoning trajectories. More recent approaches consider diversity at a global level. Chen et al. (2025c) and Walder & Karkhanis (2025) leverage pass@k as a training signal to encourage multiple candidate solutions, while, in a concurrent work, Cui et al. (2025) train a partitioning classifier to measure and amplify diversity in the advantage function. Closely related, some approaches (Chen et al., 2025b; Li et al., 2025; Hu et al., 2025) promotes global diversity among candidate solutions to improve deep exploration. However, above methods treat global and local diversity signals largely independently and do not specify how diversity at different scales should interact during optimization. In contrast, DSDR explicitly decomposes diversity into global and local components and couples them through a global-to-local allocation mechanism, which adaptively concentrates local entropy regularization on more distinctive correct reasoning trajectories.

3. Methodology

3.1. Preliminaries

We briefly review Group Relative Policy Optimization (GRPO) (Guo et al., 2025), which serves as the optimization backbone for reinforcement learning with verifiable rewards (RLVR) in reasoning tasks. Given an input prompt q , a policy π_θ generates an output sequence $o = (o_1, \dots, o_T)$ following autoregressive factorization

$$\pi_\theta(o | q) = \prod_{t=1}^T \pi_\theta(o_t | q, o_{<t}). \quad (1)$$

A verifier provides a scalar reward $r = R(q, o)$ for the completed sequence, which is typically binary for verifiable reasoning tasks. GRPO samples a group of G candidate outputs $\{o_i\}_{i=1}^G$ from a lagged behavior policy $\pi_{\theta_{\text{old}}}$ and computes rewards $\{r_i\}_{i=1}^G$. To obtain a group-relative learning signal, rewards are normalized within each group to form advantages. Specifically, the advantage A_i for each response is computed as

$$A_i = \frac{r_i - \text{mean}(r_1, r_2, \dots, r_G)}{\text{std}(r_1, r_2, \dots, r_G)}, \quad (2)$$

where $\{r_i\}_{i=1}^G$ are rewards from the group and $\text{std}(\cdot)$ denotes the standard deviation with a small constant added for numerical stability. Optimization is performed using a PPO-style clipped surrogate objective at the token level. Let T_i denote the length of o_i , and define the token-wise importance ratio $\rho_{i,t} = \pi_\theta(o_{i,t} | q, o_{i,<t}) / \pi_{\theta_{\text{old}}}(o_{i,t} | q, o_{i,<t})$.

The GRPO objective is then given by

$$J_{\text{GRPO}}(\theta) = \mathbb{E}_q \left[\frac{1}{G} \sum_{i=1}^G \frac{1}{T_i} \sum_{t=1}^{T_i} \min(\rho_{i,t} A_i, \text{clip}(\rho_{i,t}, 1 - \epsilon_c, 1 + \epsilon_c) A_i) \right] - \beta D_{\text{KL}}(\pi_\theta(\cdot | q) \| \pi_{\text{ref}}(\cdot | q)). \quad (3)$$

where ϵ_c denotes the clipping threshold, β controls the KL regularization strength, and π_{ref} is a fixed reference policy. GRPO leverages relative comparisons within each group to stabilize optimization, but its learning signal critically depends on reward variation across sampled trajectories.

3.2. DSDR: Dual-Scale Diversity Regularization

We adopt the group-based RLVR training protocol defined earlier: for each prompt q , we sample a group of G rollouts $\{o_i\}_{i=1}^G \sim \pi_{\theta_{\text{old}}}(\cdot | q)$ and obtain verifiable rewards $r_i \in \{0, 1\}$. DSDR augments the backbone with two diversity regularizers that operate at different scales and are explicitly coupled, as shown in Figure 2. At the **global (trajectory) scale**, DSDR assigns extra credit to *correct* solutions that are more distinct within the group, which keeps the learning signal informative even when many rollouts are correct and prevents premature convergence to a single reasoning template. At the **local (token) scale**, DSDR encourages controlled entropy along positive trajectories to avoid the typical *correct-mode collapse* where the model becomes highly confident token-by-token and loses nearby correct variants. The coupling is key: global distinctiveness determines where local entropy should be strongest, so local regularization expands probability mass around unique correct paths rather than uniformly perturbing all positives.

3.2.1. GLOBAL-SCALE DIVERSITY SIGNALS

For each rollout o_i in a group $\{o_1, \dots, o_G\}$, we compute a bounded per-response diversity score $d(o_i) \in [0, 1]$. The design goal is pragmatic: (i) it should reflect *trajectory-level* differences (not merely token noise), (ii) it should be *cheap* relative to rollout generation, and (iii) it should be *well-scaled* so it can be safely mixed into RLVR rewards without dominating correctness. We use two coupling signals.

Semantic Level. Let f_ϕ be a frozen text encoder that maps a full response o_i to a vector $z_i \in \mathbb{R}^d$. We normalize embeddings so that cosine similarity becomes a stable inner product:

$$z_i = f_\phi(o_i), \quad \bar{z}_i = \frac{z_i}{\|z_i\|_2}. \quad (4)$$

Given two responses o_i, o_j , we define their embedding dissimilarity via cosine distance. We scale it into $[0, 1]$ to make it numerically comparable with other bounded components:

$$\tilde{d}^{\text{emb}}(o_i, o_j) = \frac{1 - \bar{z}_i^\top \bar{z}_j}{2} \in [0, 1]. \quad (5)$$

The intuition is simple: if two responses encode similar reasoning semantics, their embeddings align and \tilde{d}^{emb} is small; if they represent different solution directions, similarity drops and the distance increases. To turn pairwise distances into a per-response score, we use the group-average dissimilarity:

$$D_{\text{emb}}(o_i) = \frac{1}{G-1} \sum_{j \neq i} \tilde{d}^{\text{emb}}(o_i, o_j). \quad (6)$$

This aggregation matters for optimization stability. A single most different neighbor can be noisy; averaging across $G-1$ comparisons yields a smoother signal that is less sensitive to an outlier rollout. Computationally, Eq. (6) is efficient: with $\bar{Z} = [\bar{z}_1, \dots, \bar{z}_G] \in \mathbb{R}^{G \times d}$, all pairwise similarities are obtained via a single matrix product $\bar{Z} \bar{Z}^\top$ followed by an elementwise transform.

Formula Level. Semantic similarity alone can miss an important axis of reasoning variation in math tasks: two solutions may appear similar at the surface level while relying on different symbolic manipulations, or vice versa. To capture this aspect, we introduce an Formula-level uniqueness signal, following the prior work (Wu et al., 2024; Chen et al., 2025b; Hu et al., 2025) while adopting a formulation aligned with our group-based setting. Let $S(o_i)$ denote the set of extracted mathematical expressions appearing in response o_i . For each formula $f \in S(o_i)$, we define a binary indicator that measures whether f is unique relative to the rest of the group:

$$\mathbb{I}_{\text{uniq}}(f, o_i) = \mathbb{1} \left[f \notin \bigcup_{j \neq i} S(o_j) \right]. \quad (7)$$

The equational diversity of response o_i is then computed as the average uniqueness of its constituent formulas:

$$D_{\text{eq}}(o_i) = \begin{cases} \frac{1}{|S(o_i)|} \sum_{f \in S(o_i)} \mathbb{I}_{\text{uniq}}(f, o_i), & |S(o_i)| > 0, \\ 0, & \text{otherwise.} \end{cases} \quad (8)$$

This definition is intentionally conservative: responses that contain no detectable formulas contribute no equational novelty. When formulas are present, the averaging form encourages structural diversity in symbolic reasoning while remaining invariant to non-mathematical paraphrasing.

Combined Global Diversity. Both components are bounded in $[0, 1]$, so we combine them into a single global diversity score by simple averaging:

$$d(o_i) = \frac{1}{2} (D_{\text{emb}}(o_i) + D_{\text{eq}}(o_i)). \quad (9)$$

This combination yields a bounded and well-scaled scalar signal for reward shaping across diverse reasoning tasks.

The embedding-based component captures trajectory-level semantic differences broadly, while the equation-based component provides a complementary, paraphrase-robust notion of novelty when symbolic manipulations are present.

Correct-Only Global Diversity Reward. We incorporate global-level diversity into RLVR only when it is consistent with the task objective. In particular, we avoid the failure case where responses are rewarded for being different despite incorrect reasoning. Accordingly, DSDR applies diversity shaping exclusively to positive rollouts and explicitly limits its influence. To prevent reward hacking (Pan et al., 2022) and avoid the diversity signal overpowering correctness, we apply a clipped technique (Sullivan et al., 2023; Li et al., 2023) only to correct rollouts and define the augmented reward as

$$\tilde{r}_i = r_i + \lambda_d \bar{d}_i \mathbb{1}(r_i = 1), \quad \bar{d}_i = \text{clip}(d(o_i); 0, \sigma_d). \quad (10)$$

Where $\lambda_d \geq 0$ controls the bonus strength and σ_d bounds the contribution of the diversity term. Equation (10) addresses a concrete optimization issue in group-relative methods: when many rollouts are correct, verifier rewards can become nearly constant within a group, shrinking reward variance and weakening within-group preference gradients. By introducing controlled dispersion among correct solutions, DSDR preserves a meaningful learning signal that differentiates alternative correct trajectories without creating incentives to explore incorrect ones. A formal statement and proof are provided in Appendix C.4.

3.2.2. GLOBAL-TO-LOCAL COUPLING OVER CORRECT TRAJECTORIES

Global diversity should not only determine which correct solutions are reinforced, but also where local entropy regularization is most effective. Intuitively, if a correct trajectory is already redundant within the group, expanding its neighborhood adds little coverage. In contrast, when a trajectory is globally distinctive, local expansion around it helps populate underexplored regions of the correct solution manifold. Let $\mathcal{P} = \{i \in [G] \mid r_i = 1\}$ denote the set of correct rollouts. We allocate local regularization strength via a diversity-weighted softmax over correct responses:

$$w_i = \begin{cases} \frac{\exp(\tau \bar{d}_i)}{\sum_{j \in \mathcal{P}} \exp(\tau \bar{d}_j)}, & i \in \mathcal{P}, \\ 0, & i \notin \mathcal{P}, \end{cases} \quad (11)$$

where $\tau > 0$ is a temperature parameter. This construction defines a probability distribution over correct rollouts (i.e., $\sum_i w_i = 1$ when $\mathcal{P} \neq \emptyset$). As τ increases, the allocation concentrates on the most globally distinctive correct solutions; as $\tau \rightarrow 0$, it reduces to uniform weighting across correct solutions. This allocation view unifies DSDR’s

dual-scale regularization: global diversity measures inter-trajectory novelty, while local entropy concentrates exploration within trajectories where novelty is highest. Theoretically, this diversity-softmax coupling can be derived as the self-normalized policy-gradient weighting induced by a correct-only, diversity-tilted objective, as claimed in Theorem 3.1 and Appendix C.6. A further principled optimality analysis of this softmax allocation is given in Appendix C.5.

3.2.3. LOCAL POSITIVE-SAMPLE REGULARIZATION

A direct way to promote diversity is to encourage high entropy in the model’s output distribution. However, for long-form generation, response-level entropy is confounded by length: longer outputs naturally accumulate more token-level uncertainty, so higher entropy may partially reflect more tokens. DSDR instead adopts *token-level conditional entropy*, averaged over timesteps (Agarwal et al., 2025; Cui et al., 2025), so that the objective measures per-step uncertainty rather than length accumulation. Let $o = (o_1, \dots, o_T) \sim \pi_{\theta_{\text{old}}}(\cdot \mid q)$. We start from the time-averaged conditional entropy:

$$J_{\text{ent}}(\theta) = \mathbb{E}_{q, o \sim \pi_{\theta_{\text{old}}}(\cdot \mid q)} \left[\frac{1}{T} \sum_{t=1}^T \mathcal{H}(\pi_{\theta}(\cdot \mid q, o_{<t})) \right]. \quad (12)$$

Using $\mathcal{H}(\pi) = -\mathbb{E}_{a \sim \pi}[\log \pi(a)]$, each entropy term can be written as an expectation of $\log \pi_{\theta}(\cdot)$. The remaining practical issue is that rollouts are sampled from $\pi_{\theta_{\text{old}}}$, while the inner expectation is taken under π_{θ} . We therefore re-express the inner expectation using standard importance sampling (Precup et al., 2000; Sheng et al., 2025b; Yao et al., 2025), allowing it to be estimated from the observed tokens o_t without resampling:

$$\mathbb{E}_{a \sim \pi_{\theta}(\cdot \mid s)}[g(a)] = \mathbb{E}_{a \sim \pi_{\theta_{\text{old}}}(\cdot \mid s)} \left[\frac{\pi_{\theta}(a \mid s)}{\pi_{\theta_{\text{old}}}(a \mid s)} g(a) \right]. \quad (13)$$

Applied at each timestep with $s = (q, o_{<t})$ and $g(a) = \log \pi_{\theta}(a \mid s)$, this yields a tractable surrogate objective that is differentiable with respect to θ while reusing group-sampled rollouts. For each group rollout $o_i = (o_{i,1}, \dots, o_{i,T_i})$, we define the per-token importance ratio:

$$\rho_{i,t} = \frac{\pi_{\theta}(o_{i,t} \mid q, o_{i,<t})}{\pi_{\theta_{\text{old}}}(o_{i,t} \mid q, o_{i,<t})}. \quad (14)$$

DSDR then defines the local objective as

$$J_{\text{local}}(\theta) = \mathbb{E} \left[- \sum_{i=1}^G \mathbb{1}(r_i = 1) w_i \frac{1}{T_i} \sum_{t=1}^{T_i} \rho_{i,t} g(o_{i,t}) \right], \quad (15)$$

where $g(a) = \log \pi_{\theta}(a \mid q, o_{<t})$. The formulation reflects three deliberate choices. Time averaging removes incentives to increase length solely to amplify the regularizer,

yielding a per-decision signal. Restricting the objective to correct rollouts ensures that local entropy refines correct trajectories rather than encouraging noise on incorrect ones. The allocation weight w_i couples local and global scales, so globally distinctive solutions receive stronger local regularization, focusing exploration on underrepresented reasoning modes. Furthermore, an information-theoretic decomposition and correctness-preservation guarantee under bounded local regularization are given in Appendix C.2.

3.2.4. DSDR OBJECTIVE

Let $J_{\text{GRPO}}(\theta; \tilde{r})$ denote the group-relative policy optimization objective defined earlier, computed using the augmented rewards \tilde{r}_i from Eq. (10) when forming group advantages. DSDR optimizes

$$J_{\text{DSDR}}(\theta) = J_{\text{GRPO}}(\theta; \tilde{r}) + \lambda_\ell J_{\text{local}}(\theta), \quad (16)$$

where $\lambda_\ell \geq 0$ controls the strength of local regularization. Eq. (16) makes the dual-scale structure explicit: the global term induces preferences among correct trajectories, while the local term mitigates token-level collapse around them, jointly enabling broad exploration with stable behavior within the correct set.

Theorem 3.1 (Diversity-tilted policy gradient induces DSDR global-to-local softmax coupling). *Fix a prompt q . Let $\bar{d}(q, o) \in [0, \sigma_d]$ denote a bounded (clipped) global diversity score for a completed rollout o (e.g., Eq. (10)), and let $R(q, o) \in \{0, 1\}$ be the verifiable reward. For $\tau > 0$, define the correct-only diversity-tilted objective*

$$\begin{aligned} J_\tau(\theta; q) &= \frac{1}{\tau} \log Z_\tau(\theta; q), \\ Z_\tau(\theta; q) &= \mathbb{E}_{o \sim \pi_\theta(\cdot | q)} [\exp(\tau \bar{d}(q, o)) \mathbb{1}(R(q, o) = 1)]. \end{aligned} \quad (17)$$

Assume $Z_\tau(\theta; q) > 0$. Then the policy gradient of J_τ admits the form

$$\nabla_\theta J_\tau(\theta; q) = \mathbb{E}_{o \sim \pi_\theta(\cdot | q)} [A_\tau^\theta(q, o) \nabla_\theta \log \pi_\theta(o | q)], \quad (18)$$

where the diversity-tilted advantage is

$$A_\tau^\theta(q, o) = \frac{1}{\tau} \left(\frac{\exp(\tau \bar{d}(q, o)) \mathbb{1}(R(q, o) = 1)}{Z_\tau(\theta; q)} - 1 \right). \quad (19)$$

Moreover, given i.i.d. rollouts $\{o_i\}_{i=1}^G \sim \pi_\theta(\cdot | q)$ with rewards $r_i = R(q, o_i)$, the self-normalized Monte Carlo form of (18) assigns weights

$$\hat{w}_i = \frac{\exp(\tau \bar{d}_i) \mathbb{1}(r_i = 1)}{\sum_{j=1}^G \exp(\tau \bar{d}_j) \mathbb{1}(r_j = 1)}, \quad (20)$$

which reduces to a diversity-softmax over correct rollouts: $\hat{w}_i \propto \exp(\tau \bar{d}_i)$ on $\mathcal{P} = \{i : r_i = 1\}$, matching DSDR’s coupling rule in Eq. (11).

4. Experiments

4.1. Experiment Settings

Backbone Models. For fair comparison, we conduct all experiments on the filtered DAPO-Math-17K (Hugging Face, 2025), which removes the duplicated samples. Training is performed on four base models with increasing capacity: Qwen2.5-Math-1.5B (Yang et al., 2024), Qwen3-1.7B and 4B (Yang et al., 2025). We adopt all-MiniLM-L6-v2 (Reimers & Gurevych, 2019) as a lightweight sentence encoder for extracting response embeddings.

Training Setting. We use the same training configuration for all models. The batch size is 256, with 8 rollouts per prompt during policy optimization and a learning rate of $1e-6$. The maximum response length is set to 4096 for Qwen2.5-Math-1.5B and 8192 for Qwen3-1.7B and Qwen3-4B in our experiment setting.

Evaluation Setting. Evaluation is conducted on a diverse set of mathematical reasoning benchmarks, including AIME2024 (Zhang & Math-AI, 2024) and AIME2025, MATH500 (Cobbe et al., 2021), Minerva Math (Lewkowycz et al., 2022), and Olympiad-level problems (He et al., 2024). For each benchmark, we report pass@1, computed from a single rollout per problem, and Avg@16, computed by averaging correctness over 16 independent rollouts. Avg@16 reflects the overall quality and stability of the model’s sampling distribution under a fixed sampling budget. In addition, we evaluate Pass@k for $k \in \{2, 4, \dots, 64\}$ by sampling 64 independent rollouts per problem. We compare our method with GRPO (Shao et al., 2024), DAPO (Yu et al., 2025) and the corresponding base models.

4.2. Main Results

Overall Performance. Our main experimental results are summarized in Table 1, covering five representative math reasoning benchmarks across three model scales. Overall, DSDR consistently outperforms all compared baselines, including Backbone, GRPO, and DAPO, demonstrating robust and scalable improvements in both Pass@1 and Avg@16 accuracy. On Qwen2.5-Math-1.5B, DSDR achieves the best average performance (25.4 / 25.6), with clear gains on challenging benchmarks such as AIME24, MATH500, and Minerva, where multiple valid reasoning paths exist. These improvements suggest that DSDR better preserves informative learning signals under group-relative optimization by differentiating correct trajectories, mitigating the reward-variance collapse that arises when many rollouts are correct. The advantage of DSDR becomes more pronounced as model scale increases. On Qwen3-1.7B and Qwen3-4B, DSDR achieves 36.8 / 36.8 and 48.0 / 46.8 average performance respectively, substantially outperforming both GRPO and DAPO at each scale, with especially large margins on AIME24 and AIME25. Importantly, DSDR consistently

DSDR: Dual-Scale Diversity Regularization for Exploration in LLM Reasoning

Table 1. Results on different reasoning benchmarks. We report **Pass@1** and **Avg@16** (%) accuracy across different model scales. DSDR consistently outperforms Backbone, GRPO, and DAPO across most benchmarks and achieves the best average performance. Ablation results (w/o GD, w/o GC) show consistent performance drops, suggesting that both global diversity (GD) and global-to-local coupling (GC) regularization play important roles in DSDR.

Models	AIME24	AIME25	MATH500	Minerva	Olympiad	Average
Qwen2.5-math-1.5B , Max Response Length = 4K tokens						
Backbone	10.0 / 3.0	3.3 / 3.0	27.4 / 21.0	5.9 / 3.9	13.1 / 9.9	11.9 / 8.2
GRPO	16.7 / 15.2	3.5 / 8.5	57.8 / 58.3	14.0 / 15.0	24.0 / 22.9	23.2 / 24.0
DAPO	13.3 / 14.4	6.7 / 6.3	54.8 / 55.3	15.8 / 15.2	22.7 / 21.4	22.7 / 22.5
DSDR	20.0 / 18.8	6.7 / 10.2	59.0 / 57.5	18.0 / 18.0	23.1 / 23.7	25.4 / 25.6
Qwen3-1.7B , Max Response Length = 8K tokens						
Backbone	13.3 / 10.6	10.0 / 7.3	57.6 / 56.5	17.3 / 17.5	23.7 / 25.3	24.4 / 23.4
GRPO	16.7 / 21.0	20.0 / 15.8	57.4 / 60.7	18.4 / 19.9	29.5 / 31.2	28.4 / 29.7
DAPO	20.0 / 20.4	10.0 / 21.0	63.8 / 64.0	21.3 / 22.3	32.9 / 32.9	29.6 / 32.1
DSDR	36.7 / 32.1	23.2 / 27.3	64.4 / 65.4	23.3 / 23.4	36.4 / 36.0	36.8 / 36.8
w/o GD	23.3 / 20.6	13.3 / 19.0	61.6 / 63.5	20.6 / 21.4	29.8 / 32.5	29.7 / 31.4
w/o GC	30.0 / 26.5	23.3 / 24.0	63.0 / 64.6	23.5 / 23.4	35.9 / 36.1	35.1 / 34.9
Qwen3-4B , Max Response Length = 8K tokens						
Backbone	13.33 / 20.63	16.67 / 16.04	64.8 / 65.75	26.10 / 24.61	32.79 / 32.69	30.74 / 31.94
GRPO	36.67 / 37.50	33.33 / 35.21	64.0 / 63.83	25.00 / 23.62	37.54 / 37.70	39.31 / 39.57
DAPO	33.33 / 38.38	40.00 / 33.13	59.0 / 62.74	25.74 / 27.37	36.65 / 39.42	38.94 / 40.21
DSDR	56.67 / 52.08	50.00 / 46.46	66.2 / 66.18	26.84 / 27.87	40.36 / 42.43	48.01 / 46.80
w/o GD	46.67 / 45.00	43.33 / 40.42	63.6 / 64.74	26.47 / 27.44	40.65 / 41.20	44.14 / 43.76
w/o GC	26.67 / 44.38	23.33 / 35.63	58.0 / 62.78	20.21 / 24.59	33.98 / 40.60	32.04 / 41.20

improves Avg@16 alongside Pass@1, indicating that the gains are not driven by occasional lucky samples but by systematically expanding the diversity of correct reasoning trajectories. Across scales, by promoting exploration exclusively within the correct solution space, DSDR enables more effective and stable exploration in RL-based LLM reasoning, leading to consistent and scalable performance gains.

Performance on Pass@k Evaluation. Figure 3 presents the pass@k performance for $k \in \{2, 4, \dots, 64\}$ across our method, DAPO and the base model Qwen3-1.7B, qwen3-4B on five benchmarks. Overall, DSDR consistently outperforms the base model and DAPO across a wide range of k, with the most pronounced gains observed on AIME2024, AIME2025, and Olympiad. On these benchmarks, the performance gap between DSDR and the baselines continues to widen as k increases, indicating that DSDR effectively expands the set of correct reasoning trajectories rather than merely sharpening a single dominant solution. On Minerva, where baseline pass@k values are relatively low and correct solutions are sparse, the absolute gains are more modest; nevertheless, DSDR maintains a consistent advantage over both the base model and DAPO across k, suggesting improved exploration even in low-reward regimes. On MATH500, where baseline accuracy is already high, DSDR delivers stable improvements across all k without satura-

tion or degradation at large k. Importantly, DSDR does not exhibit performance drop-offs at high k, highlighting its ability to promote exploration within the correct solution space rather than drifting toward noisy or incorrect samples. These results demonstrate that DSDR yields more reliable and scalable improvements in pass@k.

4.3. Ablation Study

We conduct ablation studies on Qwen3-1.7B and 4B. Table 1 reports Avg@16 and Pass@1 for variants without global diversity (GD) and without global-to-local coupling (GC). Removing global diversity causes a clear drop in average performance across benchmarks and model sizes (1.7B and 4B), indicating that trajectory-level diversity is necessary to preserve informative learning signals when many rollouts are correct and verifier rewards saturate. Removing global-to-local coupling also degrades performance, with larger drops on AIME and Olympiad, where discovering multiple valid reasoning strategies is critical. This shows that local entropy alone is insufficient; instead, local regularization must be guided by global distinctiveness to expand under-explored correct trajectories. Overall, the ablations confirm that GD and GC are complementary: GD differentiates correct solutions at the trajectory level, while GC focuses local exploration, jointly enabling the consistent gains of DSDR.

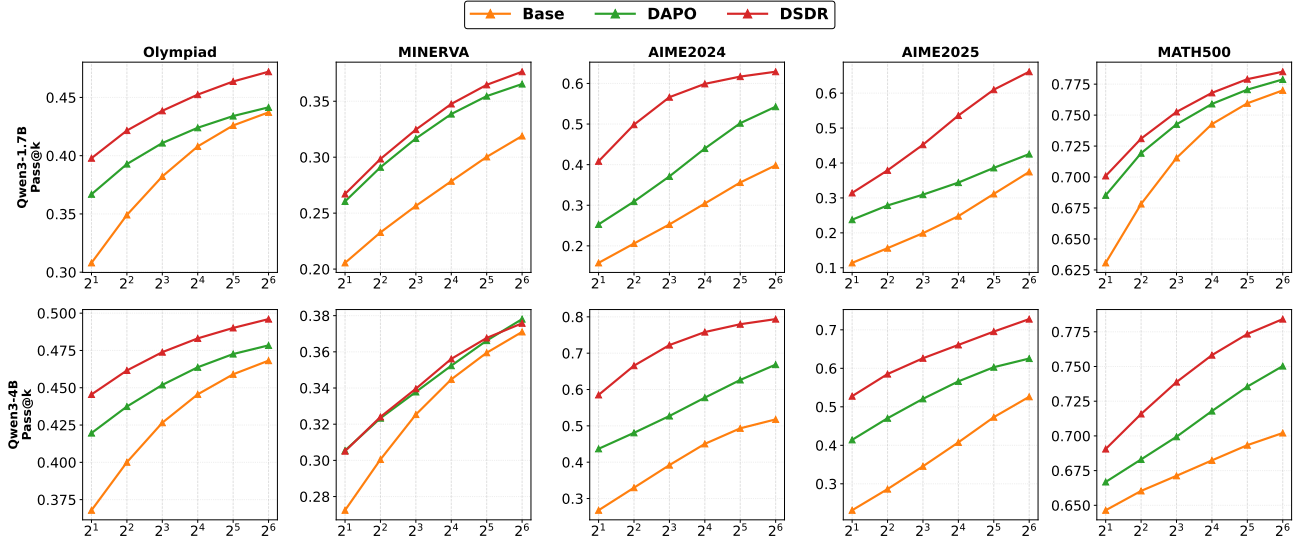


Figure 3. Pass@k performance across five benchmarks for both Qwen3-1.7B and Qwen3-4B. The Base models serve as backbones. DSDR consistently outperforms both the Base models and DAPO across all values of k .

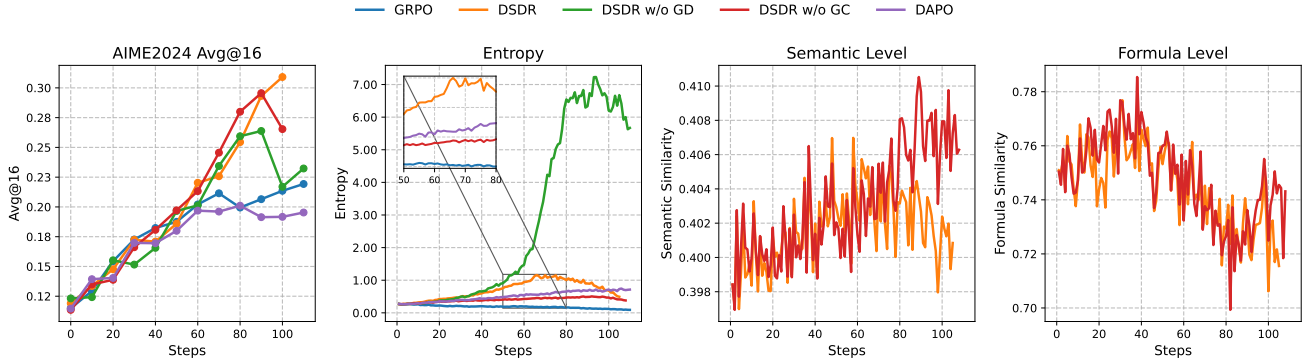


Figure 4. Training dynamics across methods conducted on Qwen3-1.7 model. From left to right, we report AIME2024 Avg@16, policy entropy, semantic-level diversity similarity, and formula-level diversity similarity. Results are shown for GRPO, DSDR, DSDR w/o GD, DSDR w/o GC, and DAPO.

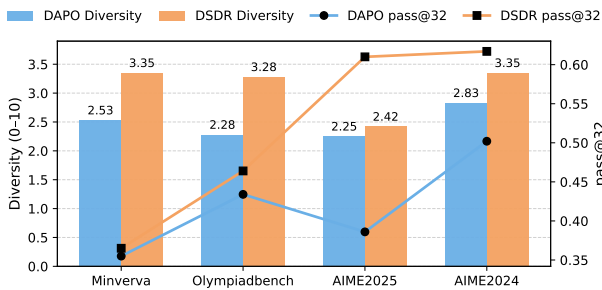


Figure 5. We generate 32 test-time rollouts per problem on four benchmarks and evaluate response diversity using an LLM-as-a-Judge (1–10 scale). The figure reports diversity scores and corresponding pass@32 for DAPO and DSDR.

4.4. Training Dynamics Analysis

Figure 4 shows the training dynamics of DSDR vs. other methods. As training progresses, DSDR achieves consistently higher Avg@16 than GRPO and DAPO on

AIME2024, indicating that DSDR improves performance while simultaneously enhancing exploration, preventing the policy from collapsing into a single dominant reasoning pattern. The entropy dynamics further highlight the role of DSDR’s dual-scale design: DSDR w/o GD exhibits a rapid and excessive increase in entropy, reflecting uncontrolled random exploration without global diversity guidance, while DSDR w/o GC, which removes token-level entropy regularization, shows diminishing exploration capacity in later stages as the policy becomes overly concentrated. In contrast, GRPO and DAPO maintain relatively low and flat entropy, suggesting limited exploration. By combining correct-only global diversity (GD) with global-to-local coupling (GC), DSDR achieves a balanced entropy profile that increases exploration without instability. This effect is further reflected in the semantic- and formula-level similarity curves, where DSDR maintains lower semantic similarity and sustained symbolic diversity among rollouts

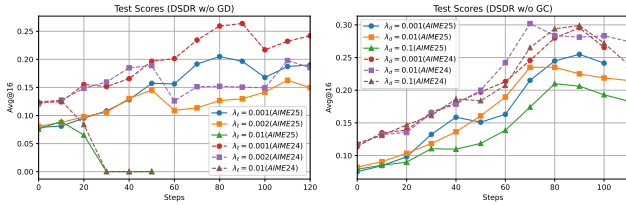


Figure 6. Hyperparameter sensitivity of DSDR on Qwen3-1.7B. Left: varying λ_ℓ shows that overly large entropy regularization destabilizes training. Right: $\lambda_d = 0.001$ achieves the best and most stable Avg@16 performance on AIME2024/2025.

throughout training, indicating that the model continues to explore multiple distinct reasoning trajectories while preserving correctness. Together, these dynamics demonstrate that DSDR enables stable and targeted exploration, preventing both random drift and premature mode collapse.

4.5. Diversity Analysis

Figure 5 compares response diversity and pass@32 across four benchmarks using 32 test-time rollouts. We use GPT-5.2 (Singh et al., 2025) to evaluate the diversity, which aggregates semantic, logical, and formula-level differences, scored on a 1–10 scale. The diversity judge prompt is provided in Appendix B.3. As shown in the figure, DSDR consistently produces higher diversity scores than DAPO across all datasets, indicating that its generated responses cover a broader range of reasoning strategies rather than collapsing into similar solution patterns. Importantly, these diversity gains are accompanied by higher pass@32 performance, demonstrating that increased diversity does not come at the cost of correctness. It indicates that by applying correct-only global diversity regularization, DSDR encourages distinct correct trajectories, while the global-to-local coupling further expands locally around the most distinctive solutions instead of injecting uniform randomness. As a result, DSDR is able to improve exploration as well as performance, yielding both higher-quality diversity and stronger pass@k performance compared to DAPO.

4.6. Hyperparameter Sensitivity of λ_ℓ and λ_d

We study the sensitivity of DSDR to the local coefficient λ_ℓ and global diversity factor λ_d on Qwen3-1.7B (Figure 6). For $\lambda_\ell \in \{0.001, 0.002, 0.01\}$, moderate regularization improves performance, while values larger than 0.01 cause training instability and collapse, indicating that excessive entropy-driven exploration disrupts correctness-aligned optimization. $\lambda_\ell = 0.001$ yields the most stable and consistently strong results and is used in our main experiments. For λ_d , we observe that 0.001 achieves the best average performance on AIME2024 and AIME2025 with stable training dynamics, whereas larger values introduce additional variance without consistent gains. We therefore adopt

$\lambda_d = 0.001$ as the default setting. Overall, DSDR remains stable within a reasonable regularization range.

5. Conclusion

In this paper, we introduced **DSDR**, a correctness-aligned dual-scale diversity regularization framework for RLVR that improves exploration in LLM reasoning. DSDR promotes *global* diversity among *correct* trajectories to sustain multiple solution modes, and applies a *local*, length-invariant token-level entropy regularizer exclusively to correct trajectories to prevent intra-mode entropy collapse. A global-to-local allocation mechanism tightly couples the two scales, focusing local regularization on globally distinctive correct trajectories. Our analysis shows that bounded local regularization preserves correctness while correct-only global shaping maintains informative learning signals under group-based optimization. Experiments across diverse reasoning benchmarks demonstrate consistent gains in accuracy, pass@k, and training stability, underscoring the importance of coordinating trajectory- and token-level exploration in RLVR for stable and robust policy optimization.

6. Impact Statements

This work introduces DSDR, a dual-scale diversity regularization framework for reinforcement learning with verifiable rewards (RLVR) in large language model (LLM) reasoning. By promoting correctness-aligned exploration at both trajectory and token levels, DSDR aims to improve reasoning robustness, stability, and sample efficiency. The proposed approach is intended to support the development of more reliable reasoning-oriented LLMs, with potential benefits for applications that require multi-step decision making and formal reasoning.

References

- Agarwal, S., Zhang, Z., Yuan, L., Han, J., and Peng, H. The unreasonable effectiveness of entropy minimization in llm reasoning. *arXiv preprint arXiv:2505.15134*, 2025.
- Boyd, S. and Vandenberghe, L. *Convex optimization*. Cambridge university press, 2004.
- Chen, L., Han, X., Wang, Q., Han, B., Bai, J., Schutze, H., and Wong, K.-F. Eepo: Exploration-enhanced policy optimization via sample-then-forget, 2025a. URL <https://arxiv.org/abs/2510.05837>.
- Chen, Y., Chakraborty, S., Wolf, L., Paschalidis, Y., and Pacchiano, A. Post-training large language models for diverse high-quality responses. *arXiv preprint arXiv:2509.04784*, 2025b.
- Chen, Z., Qin, X., Wu, Y., Ling, Y., Ye, Q., Zhao, W. X.,

- and Shi, G. Pass@k training for adaptively balancing exploration and exploitation of large reasoning models. *arXiv preprint arXiv:2508.10751*, 2025c.
- Cobbe, K., Kosaraju, V., Bavarian, M., Chen, M., Jun, H., Kaiser, L., Plappert, M., Tworek, J., Hilton, J., Nakano, R., et al. Training verifiers to solve math word problems. *arXiv preprint arXiv:2110.14168*, 2021.
- Comanici, G., Bieber, E., Schaeckermann, M., Pasupat, I., Sachdeva, N., Dhillon, I., Blistein, M., Ram, O., Zhang, D., Rosen, E., et al. Gemini 2.5: Pushing the frontier with advanced reasoning, multimodality, long context, and next generation agentic capabilities. *arXiv preprint arXiv:2507.06261*, 2025.
- Cover, T. M. *Elements of information theory*. John Wiley & Sons, 1999.
- Cui, G., Zhang, Y., Chen, J., Yuan, L., Wang, Z., Zuo, Y., Li, H., Fan, Y., Chen, H., Chen, W., et al. The entropy mechanism of reinforcement learning for reasoning language models. *arXiv preprint arXiv:2505.22617*, 2025.
- Gandhi, K., Chakravarthy, A., Singh, A., Lile, N., and Goodman, N. D. Cognitive behaviors that enable self-improving reasoners, or, four habits of highly effective stars. *arXiv preprint arXiv:2503.01307*, 2025.
- Guo, D., Yang, D., Zhang, H., Song, J., Wang, P., Zhu, Q., Xu, R., Zhang, R., Ma, S., Bi, X., et al. Deepseek-rl incentivizes reasoning in llms through reinforcement learning. *Nature*, 645(8081):633–638, 2025.
- He, C., Luo, R., Bai, Y., Hu, S., Thai, Z., Shen, J., Hu, J., Han, X., Huang, Y., Zhang, Y., et al. Olympiadbench: A challenging benchmark for promoting agi with olympiad-level bilingual multimodal scientific problems. In *Proceedings of the 62nd Annual Meeting of the Association for Computational Linguistics (Volume 1: Long Papers)*, pp. 3828–3850, 2024.
- Hou, Z., Lv, X., Lu, R., Zhang, J., Li, Y., Yao, Z., Li, J., Tang, J., and Dong, Y. Advancing language model reasoning through reinforcement learning and inference scaling. *arXiv preprint arXiv:2501.11651*, 2025.
- Hu, Z., Zhang, S., Li, Y., Yan, J., Hu, X., Cui, L., Qu, X., Chen, C., Cheng, Y., and Wang, Z. Diversity-incentivized exploration for versatile reasoning. *arXiv preprint arXiv:2509.26209*, 2025.
- Hugging Face. Open rl: A fully open reproduction of deepseek-rl, January 2025. URL <https://github.com/huggingface/open-rl>.
- Jaynes, E. T. Information theory and statistical mechanics. *Physical review*, 106(4):620, 1957.
- Jiang, Y., Huang, J., Yuan, Y., Mao, X., Yue, Y., Zhao, Q., and Yan, L. Risk-sensitive rl for alleviating exploration dilemmas in large language models. *arXiv preprint arXiv:2509.24261*, 2025.
- Lewkowycz, A., Andreassen, A., Dohan, D., Dyer, E., Michalewski, H., Ramasesh, V., Slone, A., Anil, C., Schlag, I., Gutman-Solo, T., et al. Solving quantitative reasoning problems with language models. *Advances in neural information processing systems*, 35:3843–3857, 2022.
- Li, M., Zhao, X., Lee, J. H., Weber, C., and Wermter, S. Internally rewarded reinforcement learning. In *International Conference on Machine Learning*, pp. 20556–20574. PMLR, 2023.
- Li, T., Zhang, Y., Yu, P., Saha, S., Khashabi, D., Weston, J., Lanchantin, J., and Wang, T. Jointly reinforcing diversity and quality in language model generations, 2025. URL <https://arxiv.org/abs/2509.02534>.
- Liu, A., Feng, B., Xue, B., Wang, B., Wu, B., Lu, C., Zhao, C., Deng, C., Zhang, C., Ruan, C., et al. Deepseek-v3 technical report. *arXiv preprint arXiv:2412.19437*, 2024.
- Liu, J., He, C., Lin, Y., Yang, M., Shen, F., and Liu, S. Etrrl: Balancing exploration and exploitation in llm test-time reinforcement learning via entropy mechanism. *arXiv preprint arXiv:2508.11356*, 2025a.
- Liu, M., Diao, S., Lu, X., Hu, J., Dong, X., Choi, Y., Kautz, J., and Dong, Y. Prorl: Prolonged reinforcement learning expands reasoning boundaries in large language models. *arXiv preprint arXiv:2505.24864*, 2025b.
- Pan, A., Bhatia, K., and Steinhardt, J. The effects of reward misspecification: Mapping and mitigating misaligned models. *arXiv preprint arXiv:2201.03544*, 2022.
- Precup, D., Sutton, R. S., and Singh, S. Eligibility traces for off-policy policy evaluation. 2000.
- Reimers, N. and Gurevych, I. Sentence-bert: Sentence embeddings using siamese bert-networks. *arXiv preprint arXiv:1908.10084*, 2019.
- Schulman, J., Wolski, F., Dhariwal, P., Radford, A., and Klimov, O. Proximal policy optimization algorithms. *arXiv preprint arXiv:1707.06347*, 2017.
- Shao, Z., Wang, P., Zhu, Q., Xu, R., Song, J., Bi, X., Zhang, H., Zhang, M., Li, Y., Wu, Y., et al. Deepseekmath: Pushing the limits of mathematical reasoning in open language models. *arXiv preprint arXiv:2402.03300*, 2024.
- Shen, H. On entropy control in llm-rl algorithms. *arXiv preprint arXiv:2509.03493*, 2025.

- Sheng, G., Zhang, C., Ye, Z., Wu, X., Zhang, W., Zhang, R., Peng, Y., Lin, H., and Wu, C. Hybridflow: A flexible and efficient rlhf framework. In *Proceedings of the Twentieth European Conference on Computer Systems*, pp. 1279–1297, 2025a.
- Sheng, Y., Huang, Y., Liu, S., Zhang, H., and Zeng, A. Espo: Entropy importance sampling policy optimization. *arXiv preprint arXiv:2512.00499*, 2025b.
- Singh, A., Fry, A., Perelman, A., Tart, A., Ganesh, A., El-Kishky, A., McLaughlin, A., Low, A., Ostrow, A., Ananthram, A., et al. Openai gpt-5 system card. *arXiv preprint arXiv:2601.03267*, 2025.
- Sullivan, R., Kumar, A., Huang, S., Dickerson, J., and Suarez, J. Reward scale robustness for proximal policy optimization via dreamerv3 tricks. *Advances in Neural Information Processing Systems*, 36:1352–1362, 2023.
- Sutton, R. S., McAllester, D., Singh, S., and Mansour, Y. Policy gradient methods for reinforcement learning with function approximation. *Advances in neural information processing systems*, 12, 1999.
- Walder, C. and Karkhanis, D. Pass@ k policy optimization: Solving harder reinforcement learning problems. *arXiv preprint arXiv:2505.15201*, 2025.
- Wan, Z., Dou, Z., Liu, C., Zhang, Y., Cui, D., Zhao, Q., Shen, H., Xiong, J., Xin, Y., Jiang, Y., et al. Srpo: Enhancing multimodal llm reasoning via reflection-aware reinforcement learning. *arXiv preprint arXiv:2506.01713*, 2025.
- Williams, R. J. Simple statistical gradient-following algorithms for connectionist reinforcement learning. *Machine learning*, 8(3):229–256, 1992.
- Wu, F., Xuan, W., Lu, X., Liu, M., Dong, Y., Harchaoui, Z., and Choi, Y. The invisible leash: Why rlvr may or may not escape its origin. *arXiv preprint arXiv:2507.14843*, 2025.
- Wu, T., Li, X., and Liu, P. Progress or regress? self-improvement reversal in post-training. *arXiv preprint arXiv:2407.05013*, 2024.
- Yang, A., Zhang, B., Hui, B., Gao, B., Yu, B., Li, C., Liu, D., Tu, J., Zhou, J., Lin, J., et al. Qwen2. 5-math technical report: Toward mathematical expert model via self-improvement. *arXiv preprint arXiv:2409.12122*, 2024.
- Yang, A., Li, A., Yang, B., Zhang, B., Hui, B., Zheng, B., Yu, B., Gao, C., Huang, C., Lv, C., et al. Qwen3 technical report. *arXiv preprint arXiv:2505.09388*, 2025.
- Yao, J., Cheng, R., Wu, X., Wu, J., and Tan, K. C. Diversity-aware policy optimization for large language model reasoning. *arXiv preprint arXiv:2505.23433*, 2025.
- Yu, Q., Zhang, Z., Zhu, R., Yuan, Y., Zuo, X., Yue, Y., Dai, W., Fan, T., Liu, G., Liu, L., et al. Dapo: An open-source llm reinforcement learning system at scale. *arXiv preprint arXiv:2503.14476*, 2025.
- Zhang, Q., Wu, H., Zhang, C., Zhao, P., and Bian, Y. Right question is already half the answer: Fully unsupervised llm reasoning incentivization. *arXiv preprint arXiv:2504.05812*, 2025.
- Zhang, Y. and Math-AI, T. American invitational mathematics examination (aime) 2024, 2024.

A. Implementation Details

We provide more details for experiments in Section 4. We provide additional experimental details in Section 4. All models are trained using the VERL framework (Sheng et al., 2025a) and deployed on $8 \times$ NVIDIA A100 GPUs (40GB). Table 2 and Table 3 summarize the training and evaluation hyperparameters. Unless otherwise specified, we adopt a rollout group size of $n = 8$, a learning rate of 1×10^{-6} , and binary verifier rewards. We conduct hyperparameter sweeps over the global diversity scaling factor $\lambda_d \in \{0.001, 0.01, 0.1\}$, the local regularization coefficient $\lambda_\ell \in \{0.001, 0.002, 0.01\}$, and the coupling temperature $\tau \in \{1, 5, 10\}$. Empirically, we find that $\lambda_d = 0.001$, $\lambda_\ell = 0.001$, and $\tau = 5$ consistently yield the best or near-best performance across benchmarks; these values are therefore used as defaults in all reported experiments.

Table 2. Summary of training details.

Training Settings	
Hardware	$8 \times$ A100 GPUs (40GB)
Base models	Qwen2.5-Math-1.5B / Qwen3-1.7B, 4B
Training dataset	open-r1/DAPO-Math-17K-Processed
Max response length	4096 / 8192
Batch / mini-batch size	256 / 16
Rollout group size n	8
Learning rate	1×10^{-6}
Temperature (training)	1.0
Clip range ($\epsilon_{\text{low}}, \epsilon_{\text{high}}$)	(0.2, 0.28) / (0.2, 0.2) for GRPO only
Reward type	Binary reward
Coupling temperature parameter τ	{1, 5, 10}
Reward scaling factor λ_d	{0.001, 0.01, 0.1}
Regularization coefficient λ_ℓ	{0.001, 0.002, 0.01}

Table 3. Evaluation settings.

Evaluation settings	
Max response length	4096 / 8192
Top- p (eval)	0.9
Temperature (eval)	0.1 for Pass@1; 0.7 for Avg@16

B. Additional Results

B.1. Additional Training Dynamics Analysis

As shown in figure 7, DSDR steadily improves both Avg@16 and Pass@16 over training, indicating that performance gains are accompanied by sustained exploration rather than convergence to a narrow solution mode. In contrast, GRPO and DAPO display slower growth and earlier saturation, suggesting limited ability to expand the set of correct solutions. And removing global diversity (w/o GD) results in large fluctuations in the policy-gradient loss, reflecting unstable learning when trajectory-level differentiation among correct rollouts is absent. On the other hand, without global-to-local coupling (w/o GC), leads to weaker late-stage improvements and a sharp increase in the clip ratio, indicating overly aggressive updates and reduced robustness as token-level exploration diminishes. By jointly enforcing correct-only global diversity and diversity-guided local regularization, DSDR maintains controlled updates and effective exploration throughout training, which translates into more reliable and higher final performance.

B.2. Case Study

In this section, we present generated samples during testing. One sample with 16 test-time rollouts, DSDR achieves 7 correct solutions, compared to only 2 for DAPO. We show two example responses generated by DSDR, which arrive at the correct answer through distinct reasoning processes, illustrating its ability to explore multiple valid solution paths. In contrast, we present two responses generated by DAPO, which exhibit more limited diversity. This demonstrates that DSDR

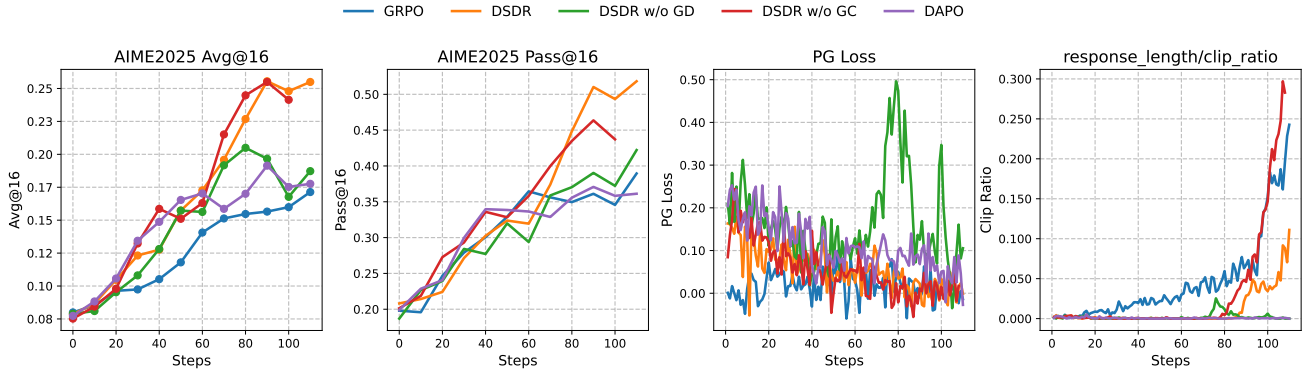


Figure 7. Training dynamics across methods conducted on Qwen3-1.7B model. From left to right, we show Avg@16 and Pass@16 for AIME2025, PG loss, and response length/clip ratio, comparing GRPO, DSDR, DSDR w/o GD, DSDR w/o GC, and DAPO.

improves exploration without sacrificing solution fidelity: by maintaining controlled diversity across rollouts, the model avoids mode collapse while consistently discovering correct reasoning paths, leading to stronger overall performance.

B.2.1. SAMPLES GENERATED BY DSDR

Two generated samples by DSDR are shown below, and the yellow boxes highlight the different solution strategies used to solve this problem.

Generated Sample: Answer 1

Problem.

Let N be the greatest four-digit positive integer with the property that whenever one of its digits is changed to 1, the resulting number is divisible by 7. Let Q and R be the quotient and remainder, respectively, when N is divided by 1000. Find $Q + R$. **Ground Truth:** 699

Answer.

We are given a four-digit number N such that whenever one of its digits is changed to 1, the resulting number is divisible by 7. We are to find $Q + R$, where $N = 1000Q + R$, and Q and R are the quotient and remainder when N is divided by 1000.

STEP 1: UNDERSTAND THE CONDITION

Let's consider all possible changes to the digits of N , and the resulting number must be divisible by 7.

Let $N = ABCD$, where A, B, C, D are digits (each from 0 to 9, with $A \neq 0$).

We must ensure that **for every digit position** (i.e., for each digit A, B, C, D), changing that digit to 1 results in a number divisible by 7.

This means:

- Changing the first digit A to 1: $1BCD$ must be divisible by 7.
- Changing the second digit B to 1: $AB1D$ must be divisible by 7.
- Changing the third digit C to 1: $ABD1$ must be divisible by 7.
- Changing the fourth digit D to 1: $ABC1$ must be divisible by 7.

So we have four divisibility conditions:

$$1BCD \equiv 0, \quad AB1D \equiv 0, \quad ABD1 \equiv 0, \quad ABC1 \equiv 0 \pmod{7}.$$

STEP 2: REPRESENT THE NUMBERS ALGEBRAICALLY

Let $N = 1000A + 100B + 10C + D$.

The four conditions become:

$$\begin{aligned} 1000 + 100B + 10C + D &\equiv 0 \pmod{7}, \\ 1000A + 100 + 10C + D &\equiv 0 \pmod{7}, \\ 1000A + 100B + 10 + D &\equiv 0 \pmod{7}, \\ 1000A + 100B + 10C + 1 &\equiv 0 \pmod{7}. \end{aligned}$$

STEP 3: USE MODULAR ARITHMETIC TO SIMPLIFY

Using

$$1000 \equiv 6, \quad 100 \equiv 2, \quad 10 \equiv 3 \pmod{7},$$

we obtain four congruences, which are then manipulated to derive relations among A, B, C, D .

STEP 4: SOLVING RELATIONS

Through successive subtraction and modular inversion, we find:

$$A = 5, \quad B = 6.$$

Solving the remaining congruences yields two admissible digit pairs:

$$(C, D) \in \{(2, 4), (9, 4)\}.$$

Each candidate is then explicitly checked by substituting back into all four digit-replacement conditions to verify divisibility by 7.

Both 5624 and 5694 satisfy the conditions. Since the problem asks for the greatest such number, we select

$$N = 5694.$$

Thus,

$$Q = 5, \quad R = 694, \quad Q + R = \boxed{699}.$$

FINAL ANSWER

$$\boxed{699}$$

Generated Sample: Answer 2

Problem.

Let N be the greatest four-digit positive integer with the property that whenever one of its digits is changed to 1, the resulting number is divisible by 7. Let Q and R be the quotient and remainder, respectively, when N is divided by 1000. Find $Q + R$. **Ground Truth:** 699

Answer.

We are given a four-digit number N , such that whenever one of its digits is changed to 1, the resulting number is divisible by 7. We are to find $Q + R$, where Q is the quotient and R is the remainder when N is divided by 1000.

STEP 1: UNDERSTANDING THE PROBLEM

We need to find the **greatest** four-digit number N such that **any single digit change to 1** results in a number divisible by 7.

Let $N = ABCD$, where A, B, C, D are digits with $A \neq 0$.

For each digit position, changing that digit to 1 must yield a number divisible by 7.

STEP 2: FORMULATING CONDITIONS

Case 1: Change the thousands digit A to 1:

$$1000 + BCD \equiv 0 \pmod{7} \Rightarrow BCD \equiv 1 \pmod{7}.$$

Case 2: Change the hundreds digit B to 1:

$$1000A + 100 + 10C + D \equiv 0 \pmod{7} \Rightarrow 6A + 3C + D \equiv 5 \pmod{7}.$$

Case 3: Change the tens digit C to 1:

$$1000A + 100B + 10 + D \equiv 0 \pmod{7} \Rightarrow 6A + 2B + D \equiv 4 \pmod{7}.$$

Case 4: Change the units digit D to 1:

$$1000A + 100B + 10C + 1 \equiv 0 \pmod{7} \Rightarrow 6A + 2B + 3C \equiv 6 \pmod{7}.$$

STEP 3: SUMMARIZE THE CONDITIONS

Using $100 \equiv 2, 10 \equiv 3 \pmod{7}$, we obtain:

$$2B + 3C + D \equiv 1 \pmod{7}.$$

Together with the other three congruences, we form a system in A, B, C, D .

STEP 4: SOLVE THE SYSTEM OF CONGRUENCES

By subtracting equations and eliminating variables, we obtain:

$$3A - B \equiv 2 \pmod{7}, \quad 3C - D \equiv 2 \pmod{7}, \quad 2B - 3C \equiv 6 \pmod{7}.$$

STEP 5: EXPRESS VARIABLES

Solving step-by-step yields:

$$A = 5, \quad B = 6,$$

and

$$C \in \{2, 9\}, \quad D = 4.$$

This branching step yields two admissible candidates:

$$N \in \{5624, 5694\}.$$

STEP 8: VERIFICATION

All four digit-replacement conditions are explicitly checked and satisfied for

$$N = 5694.$$

STEP 9: COMPUTE $Q + R$

Since $5694 = 1000 \cdot 5 + 694$, we have:

$$Q = 5, \quad R = 694, \quad Q + R = \boxed{699}.$$

FINAL ANSWER

$$\boxed{699}$$

B.2.2. SAMPLES GENERATED BY DAPO

Two samples generated by DAPO are shown below, and the red boxes highlight the erroneous solution strategies that lead to failure.

Generated Sample: Answer 1

Problem.

Let N be the greatest four-digit positive integer with the property that whenever one of its digits is changed to 1, the resulting number is divisible by 7. Let Q and R be the quotient and remainder, respectively, when N is divided by 1000. Find $Q + R$. **Ground Truth:** 699

Answer.

We are given a **four-digit number** N such that **any change of one digit to 1 results in a number divisible by 7**. Let's denote N as a four-digit number:

$$N = 1000a + 100b + 10c + d$$

Where:

- a, b, c, d are digits (integers from 0 to 9, with $a \neq 0$ since N is a four-digit number),
- $a \in \{1, 2, \dots, 9\}, b, c, d \in \{0, 1, \dots, 9\}$.

STEP 1: UNDERSTANDING THE CONDITION

The problem says: **Whenever one digit is changed to 1, the resulting number is divisible by 7**.

So, there are four different cases:

1. Change a to 1: $1000 + 100b + 10c + d$
2. Change b to 1: $1000a + 100 + 10c + d$
3. Change c to 1: $1000a + 100b + 10 + d$
4. Change d to 1: $1000a + 100b + 10c + 1$

Each must be divisible by 7, giving:

$$\begin{aligned} 1000 + 100b + 10c + d &\equiv 0 \pmod{7}, \\ 1000a + 100 + 10c + d &\equiv 0 \pmod{7}, \\ 1000a + 100b + 10 + d &\equiv 0 \pmod{7}, \\ 1000a + 100b + 10c + 1 &\equiv 0 \pmod{7}. \end{aligned}$$

Using

$$1000 \equiv 6, \quad 100 \equiv 2, \quad 10 \equiv 3 \pmod{7},$$

we obtain:

$$\begin{aligned} 2b + 3c + d &\equiv 1 \pmod{7} \quad (1) \\ 6a + 3c + d &\equiv 5 \pmod{7} \quad (2) \\ 6a + 2b + d &\equiv 4 \pmod{7} \quad (3) \\ 6a + 2b + 3c &\equiv 6 \pmod{7} \quad (4) \end{aligned}$$

We now attempt to solve this system of congruences.

Logical error starts here (unsupported assumption).

Assume $a = 1$ (the smallest possible digit, since N is a four-digit number), then try values of b, c, d that satisfy the congruences.

From this point onward, the reasoning proceeds by ad-hoc guessing and trial-based arguments that are not logically implied by the modular system above.
Eventually, the solution concludes:

$$Q = 111, \quad R = 1, \quad Q + R = 112$$

FINAL ANSWER

112

Generated Sample: Answer 2

Problem.

Let N be the greatest four-digit positive integer with the property that whenever one of its digits is changed to 1, the resulting number is divisible by 7. Let Q and R be the quotient and remainder, respectively, when N is divided by 1000. Find $Q + R$. **Ground Truth:** 699

Answer.

We are asked to find the **greatest four-digit number** N such that **if any one of its digits is changed to 1**, the resulting number is divisible by 7. Then, given $N = 1000Q + R$, we are to find $Q + R$.

STEP 1: UNDERSTAND THE CONDITION

Let's denote N as a four-digit number:

$$N = 1000a + 100b + 10c + d$$

where $a, b, c, d \in \{0, 1, \dots, 9\}$, with $a \neq 0$.

Changing each digit to 1 gives the conditions:

$$\begin{aligned} 1000 + 100b + 10c + d &\equiv 0 \pmod{7}, \\ 1000a + 100 + 10c + d &\equiv 0 \pmod{7}, \\ 1000a + 100b + 10 + d &\equiv 0 \pmod{7}, \\ 1000a + 100b + 10c + 1 &\equiv 0 \pmod{7}. \end{aligned}$$

Using

$$1000 \equiv 6, \quad 100 \equiv 2, \quad 10 \equiv 3 \pmod{7},$$

we obtain:

$$\begin{aligned} 2b + 3c + d &\equiv 1 \pmod{7}, \\ 6a + 3c + d &\equiv 5 \pmod{7}, \\ 6a + 2b + d &\equiv 4 \pmod{7}, \\ 6a + 2b + 3c &\equiv 6 \pmod{7}. \end{aligned}$$

Logical error starts here (invalid constraint assumption).

Let's suppose that all four expressions are congruent to the same value $x \pmod{7}$, and in particular, assume

$$x = 0 \quad (\text{i.e., } N \equiv 0 \pmod{7}).$$

From this point onward, the reasoning proceeds by enumerating digit values under the unsupported assumption that all four congruences must equal the same residue class, which is not implied by the original system.

The solution eventually concludes:

$$Q = 9, \quad R = 888, \quad Q + R = 897.$$

FINAL ANSWER

897

B.3. Prompt Template

Prompt Template for Diversity Scoring

System: You are a strict but fair grader. You will be given one math problem and **32 independent rollouts (solutions)**. Your task is to score diversity across rollouts.

Evaluate the following three dimensions on a **0–10 scale**:

- **logic_diversity**: differences in reasoning flow or step order
- **formula_diversity**: differences in formulas, identities, or techniques used
- **semantic_diversity**: differences in overall semantic approach or framing

Then output **overall diversity** as the average of the three scores (**0–10**, rounded to **one decimal**).

Be objective and do not prefer any model. **Output JSON only.**

C. Theoretical Analysis of DSDR

This appendix part provides formal justification for the key design choices in DSDR (Sec. 3.2): (i) the *correct-only* global diversity reward (Eq. (10)), (ii) the global-to-local coupling weights (Eq. (11)), and (iii) the *positive-only*, length-invariant token-level entropy regularizer (Eq. (15)).

C.1. Setup, Notation, and Standing Assumptions

We consider RLVR with verifiable reward on prompts $q \sim \mathcal{D}$. A policy $\pi(\cdot | q)$ induces an output random variable O (a sequence of tokens) and a verifier reward $R(q, O) \in \{0, 1\}$. For group-based training (GRPO-style), for each prompt q we sample a group $\{o_i\}_{i=1}^G$ and obtain rewards $\{r_i\}_{i=1}^G$ with $r_i = R(q, o_i)$.

Augmented Reward (Correct-Only Global Diversity Reward) For each rollout o_i , we compute a diversity score $d(o_i)$ and use a clipped score

$$\bar{d}_i = \text{clip}(d(o_i); 0, \sigma_d) \in [0, \sigma_d]. \quad (21)$$

The augmented reward used for group advantage computation is

$$\tilde{r}_i = r_i + \lambda_d \bar{d}_i \mathbb{1}(r_i = 1), \quad \lambda_d \geq 0. \quad (22)$$

Group Normalization Define the empirical mean and standard deviation of $\{\tilde{r}_i\}_{i=1}^G$:

$$\mu_{\tilde{r}} = \frac{1}{G} \sum_{i=1}^G \tilde{r}_i, \quad \sigma_{\tilde{r}} = \sqrt{\frac{1}{G} \sum_{i=1}^G (\tilde{r}_i - \mu_{\tilde{r}})^2}. \quad (23)$$

In practice we use a stabilized standard deviation $\sigma_{\tilde{r}, \varepsilon} > 0$, e.g., $\sigma_{\tilde{r}, \varepsilon} = \sigma_{\tilde{r}} + \varepsilon$ or $\sigma_{\tilde{r}, \varepsilon} = \sqrt{\sigma_{\tilde{r}}^2 + \varepsilon^2}$ with $\varepsilon > 0$. The normalized advantages are

$$\tilde{A}_i = \frac{\tilde{r}_i - \mu_{\tilde{r}}}{\sigma_{\tilde{r}, \varepsilon}}. \quad (24)$$

All results below remain valid under either stabilization choice as long as $\varepsilon > 0$.

Entropy Conventions. The action space at each decoding step is the vocabulary \mathcal{V} , assumed finite. All logarithms are natural logs. Standard entropy identities and bounds follow classical information theory (Cover, 1999).

Correctness Gap Assumption For Proposition C.2, we assume a strict gap

$$\Delta := J_R^* - \bar{J}_R > 0, \quad (25)$$

where J_R^* is optimal correctness and \bar{J}_R is the best correctness strictly below optimal. This separation commonly holds when the set of achievable correctness values is discrete under a restricted policy class.

C.2. Inter-/Intra-mode Decomposition (Formal Complementarity)

DSDR introduces *two* diversity mechanisms operating at different scales: a *global* (sequence-level) preference among correct trajectories (Eq. (10)) and a *local* (token-level) positive-only entropy regularizer (Eq. (15)). This subsection provides an information-theoretic lens clarifying why these two terms are complementary rather than redundant: global shaping targets *inter-mode* coverage (deep exploration across distinct reasoning modes), while local entropy targets *intra-mode* thickening (maintaining non-collapsed variability within a mode).

We view generation as a mixture over latent “reasoning modes” Z (e.g., distinct solution strategies). For each prompt q , suppose

$$Z \sim p(z | q), \quad O \sim p(o | z, q). \quad (26)$$

Lemma C.1 (Inter-/intra-mode entropy decomposition). *For any fixed prompt q ,*

$$H(O | q) = I(O; Z | q) + H(O | Z, q), \quad (27)$$

where $I(O; Z | q)$ is conditional mutual information.

Proof. This is a standard identity (Cover, 1999). By definition, $I(O; Z | q) = H(O | q) - H(O | Z, q)$. Rearranging yields (27). \square

Interpretation of DSDR. $I(O; Z | q)$ captures *inter-mode* diversity (deep exploration across reasoning modes), while $H(O | Z, q)$ captures *intra-mode* diversity (variation within a mode). DSDR’s global shaping primarily promotes inter-mode coverage, while local positive-only entropy discourages intra-mode collapse.

C.3. Correctness Preservation Under Bounded Local Regularization

The local objective in DSDR (Eq. (15)) increases token-level entropy *only along correct trajectories* and is length-normalized to avoid incentivizing longer outputs. A natural concern is whether adding this regularizer could sacrifice verifiable correctness. This subsection shows that, at the population level, a *sufficiently small* local regularization weight cannot make a lower-correctness policy optimal; it can only break ties among correctness-optimal policies.

Entropy Upper Bound for Length-invariant Token Entropy. For any categorical distribution over $|\mathcal{V}|$ tokens, entropy is maximized by the uniform distribution, so $0 \leq \mathcal{H}(\pi(\cdot | s)) \leq \log |\mathcal{V}|$ (Cover, 1999). Define the length-invariant per-token conditional entropy functional

$$J_H(\pi) = \mathbb{E} \left[\frac{1}{T} \sum_{t=1}^T \mathcal{H}(\pi(\cdot | q, o_{<t})) \right]. \quad (28)$$

Then

$$0 \leq J_H(\pi) \leq H_{\max} := \log |\mathcal{V}|. \quad (29)$$

The same upper bound also holds for the positive-only variant $J_H^+(\pi) = \mathbb{E}[\mathbb{1}(R(q, O) = 1) \cdot \frac{1}{T} \sum_t \mathcal{H}(\cdot)]$ since $\mathbb{1}(\cdot) \leq 1$.

Proposition C.2 (Correctness preservation under bounded λ_ℓ). *Define the population correctness objective*

$$J_R(\pi) = \mathbb{E}_{q \sim \mathcal{D}, o \sim \pi(\cdot | q)} [R(q, o)] \in [0, 1], \quad (30)$$

and let $J_R^* = \sup_{\pi} J_R(\pi)$. Define the best correctness among strictly suboptimal policies

$$\bar{J}_R = \sup_{\pi: J_R(\pi) < J_R^*} J_R(\pi), \quad \Delta := J_R^* - \bar{J}_R > 0. \quad (31)$$

Let $J_H(\pi)$ be any regularizer satisfying $0 \leq J_H(\pi) \leq H_{\max}$ (e.g., (28)). Consider the regularized objective

$$J_{\text{reg}}(\pi) = J_R(\pi) + \lambda_{\ell} J_H(\pi), \quad \lambda_{\ell} \geq 0. \quad (32)$$

If $\lambda_{\ell} < \Delta/H_{\max}$, then every maximizer $\pi_{\text{reg}}^* \in \arg \max_{\pi} J_{\text{reg}}(\pi)$ is correctness-optimal:

$$J_R(\pi_{\text{reg}}^*) = J_R^*. \quad (33)$$

Proof. Take any correctness-suboptimal policy π with $J_R(\pi) \leq \bar{J}_R$. Using $J_H(\pi) \leq H_{\max}$,

$$J_{\text{reg}}(\pi) = J_R(\pi) + \lambda_{\ell} J_H(\pi) \leq \bar{J}_R + \lambda_{\ell} H_{\max}. \quad (34)$$

Take any correctness-optimal policy π^* with $J_R(\pi^*) = J_R^*$. Since $J_H(\pi^*) \geq 0$,

$$J_{\text{reg}}(\pi^*) = J_R^* + \lambda_{\ell} J_H(\pi^*) \geq J_R^*. \quad (35)$$

If $\lambda_{\ell} < \Delta/H_{\max}$, then

$$\bar{J}_R + \lambda_{\ell} H_{\max} < \bar{J}_R + \Delta = J_R^* \leq J_{\text{reg}}(\pi^*). \quad (36)$$

Thus every correctness-suboptimal π has strictly smaller $J_{\text{reg}}(\pi)$ than some correctness-optimal π^* , so no correctness-suboptimal policy can maximize J_{reg} . Hence any maximizer satisfies (33). \square

C.4. GRPO Signal Preservation via Correct-Only Global Diversity Reward

DSDR’s augmented reward (Eq. (10)) is motivated by a concrete optimization issue in group-relative methods: when verifier rewards become nearly constant within a group (e.g., many correct rollouts), the within-group variance shrinks and the group-normalized advantages used in GRPO can degenerate. This subsection formalizes two points aligned with Sec. 3.2: (i) verifier-only rewards yield informative groups only when the sampled group mixes successes and failures, and (ii) DSDR’s correct-only diversity bonus creates controlled dispersion among correct solutions, ensuring non-degenerate group-normalized advantages whenever diversity scores differ.

Lemma C.3 (Probability of a mixed verifier-reward group). *Fix prompt q . Let r_1, \dots, r_G be i.i.d. Bernoulli(p), where*

$$p = \Pr(R(q, O) = 1). \quad (37)$$

Let $\text{Mix} = \{\exists i, j : r_i \neq r_j\}$ denote the mixed-group event. Then

$$\Pr(\text{Mix}) = P_{\text{mix}}(p; G) = 1 - p^G - (1 - p)^G. \quad (38)$$

Proof. The complement of Mix is the disjoint union of “all ones” and “all zeros”, with probabilities p^G and $(1 - p)^G$, respectively. Therefore $\Pr(\text{Mix}) = 1 - p^G - (1 - p)^G$. \square

Proposition C.4 (Non-vanishing GRPO signal under correct-only diversity bonus). *Let \tilde{r}_i be defined in (22) and \tilde{A}_i be the stabilized group-normalized advantages in (24). If there exist $i \neq j$ such that $\tilde{r}_i \neq \tilde{r}_j$, then*

$$\text{Var}(\tilde{r}_1, \dots, \tilde{r}_G) > 0 \quad \text{and} \quad \{\tilde{A}_i\}_{i=1}^G \text{ are not all zero.} \quad (39)$$

In particular, in a solve-all group ($r_i = 1$ for all i),

$$\tilde{r}_i = 1 + \lambda_d \bar{d}_i. \quad (40)$$

If $\lambda_d > 0$ and $\{\bar{d}_i\}$ are not all identical, then group-relative advantages remain non-degenerate even though verifier rewards are constant.

Proof. If \tilde{r}_i are not all identical, then letting $\mu_{\tilde{r}}$ be the group mean in (23), there exists an index i such that $\tilde{r}_i \neq \mu_{\tilde{r}}$, hence

$$\text{Var}(\tilde{r}_1, \dots, \tilde{r}_G) = \frac{1}{G} \sum_{k=1}^G (\tilde{r}_k - \mu_{\tilde{r}})^2 > 0. \quad (41)$$

Because $\sigma_{\tilde{r}, \varepsilon} > 0$ by construction, for that index i we have $\tilde{A}_i = (\tilde{r}_i - \mu_{\tilde{r}}) / \sigma_{\tilde{r}, \varepsilon} \neq 0$, so the advantages are not all zero. The solve-all case follows by substituting (40): if $\lambda_d > 0$ and \bar{d}_i are not all equal, then \tilde{r}_i are not all equal and the above applies. \square

Remark (Connection to PPO/GRPO). In PPO-style clipped surrogate objectives (Schulman et al., 2017) and GRPO-style group-relative updates (e.g., (Guo et al., 2025)), the reward-driven policy-improvement term is scaled by normalized advantages. If all advantages were zero, the reward-driven gradient would vanish (leaving only KL regularization). Proposition C.4 guarantees non-degenerate preference signal whenever diversity induces non-constant \tilde{r}_i .

C.5. Optimality of Diversity-Softmax Global-to-Local Coupling

DSDR couples global and local regularization by allocating the local entropy budget across correct trajectories according to the diversity-softmax weights (Eq. (11)). This subsection shows that the softmax allocation is not an ad-hoc heuristic: it is the unique solution of an entropy-regularized resource allocation problem. This provides a principled interpretation of the temperature τ as a concentration–exploration control knob.

Proposition C.5 (Softmax allocation optimality). *Assume $\mathcal{P} = \{i : r_i = 1\} \neq \emptyset$. Consider allocating a local-entropy budget across correct rollouts with a distribution w over \mathcal{P} :*

$$w_i \geq 0, \quad \sum_{i \in \mathcal{P}} w_i = 1. \quad (42)$$

For $\tau > 0$, the diversity-softmax weights

$$w_i^* = \frac{\exp(\tau \bar{d}_i)}{\sum_{j \in \mathcal{P}} \exp(\tau \bar{d}_j)} \quad (43)$$

are the unique maximizer of the entropy-regularized allocation problem

$$\max_{w \in \Delta(\mathcal{P})} \left(\tau \sum_{i \in \mathcal{P}} w_i \bar{d}_i + \mathcal{H}(w) \right), \quad \mathcal{H}(w) = - \sum_{i \in \mathcal{P}} w_i \log w_i, \quad (44)$$

where $\Delta(\mathcal{P})$ is the simplex in (42).

Proof. This is the classical maximum-entropy / Gibbs distribution derivation (Jaynes, 1957); we provide a convex-optimization proof via KKT conditions (Boyd & Vandenberghe, 2004).

(Uniqueness) The objective in (44) is linear in w plus entropy $\mathcal{H}(w)$, which is strictly concave over the simplex interior (Cover, 1999; Boyd & Vandenberghe, 2004). Hence the objective is strictly concave and the maximizer is unique.

(Stationarity) Form the Lagrangian with multiplier α for $\sum_{i \in \mathcal{P}} w_i = 1$:

$$\mathcal{L}(w, \alpha) = \tau \sum_{i \in \mathcal{P}} w_i \bar{d}_i - \sum_{i \in \mathcal{P}} w_i \log w_i + \alpha \left(\sum_{i \in \mathcal{P}} w_i - 1 \right). \quad (45)$$

At an interior optimum, stationarity gives

$$\frac{\partial \mathcal{L}}{\partial w_i} = \tau \bar{d}_i - (1 + \log w_i) + \alpha = 0 \quad \Rightarrow \quad \log w_i = \tau \bar{d}_i + \alpha - 1. \quad (46)$$

Exponentiating yields $w_i = C \exp(\tau \bar{d}_i)$ with $C = \exp(\alpha - 1)$. Enforcing the simplex constraint implies $C = \left(\sum_{j \in \mathcal{P}} \exp(\tau \bar{d}_j) \right)^{-1}$, yielding (43). By strict concavity, this stationary point is the unique global maximizer. \square

Equivalent KL-Regularized Form. Let u be the uniform distribution on \mathcal{P} . Using $\mathcal{H}(w) = \log |\mathcal{P}| - D_{\text{KL}}(w||u)$, the problem (44) is equivalent (up to an additive constant) to

$$\max_{w \in \Delta(\mathcal{P})} (\tau \mathbb{E}_{i \sim w} [\bar{d}_i] - D_{\text{KL}}(w||u)),$$

highlighting the exploration–concentration tradeoff controlled by τ .

C.6. Proof of Theorem 3.1

Proof. Fix q and define

$$f(q, o) = \exp(\tau \bar{d}(q, o)) \mathbb{1}(R(q, o) = 1) \geq 0.$$

By definition,

$$J_\tau(\theta; q) = \frac{1}{\tau} \log Z_\tau(\theta; q), \quad Z_\tau(\theta; q) = \mathbb{E}_{o \sim \pi_\theta(\cdot|q)} [f(q, o)].$$

Since $Z_\tau(\theta; q) > 0$ by assumption, we can differentiate:

$$\nabla_\theta J_\tau(\theta; q) = \frac{1}{\tau} \cdot \frac{1}{Z_\tau(\theta; q)} \nabla_\theta Z_\tau(\theta; q). \quad (47)$$

Using the score-function (log-derivative) identity (Williams, 1992; Sutton et al., 1999),

$$\nabla_\theta \mathbb{E}_{o \sim \pi_\theta(\cdot|q)} [f(q, o)] = \mathbb{E}_{o \sim \pi_\theta(\cdot|q)} [f(q, o) \nabla_\theta \log \pi_\theta(o | q)], \quad (48)$$

we obtain

$$\nabla_\theta Z_\tau(\theta; q) = \mathbb{E}_{o \sim \pi_\theta(\cdot|q)} [f(q, o) \nabla_\theta \log \pi_\theta(o | q)]. \quad (49)$$

Substituting (49) into (47) yields

$$\nabla_\theta J_\tau(\theta; q) = \mathbb{E}_{o \sim \pi_\theta(\cdot|q)} \left[\frac{1}{\tau} \frac{f(q, o)}{Z_\tau(\theta; q)} \nabla_\theta \log \pi_\theta(o | q) \right]. \quad (50)$$

Next, note that

$$\mathbb{E}_{o \sim \pi_\theta(\cdot|q)} [\nabla_\theta \log \pi_\theta(o | q)] = \nabla_\theta \int \pi_\theta(o | q) do = \nabla_\theta 1 = 0,$$

so subtracting the constant baseline $1/\tau$ does not change the expectation (?):

$$\nabla_\theta J_\tau(\theta; q) = \mathbb{E}_{o \sim \pi_\theta(\cdot|q)} \left[\frac{1}{\tau} \left(\frac{f(q, o)}{Z_\tau(\theta; q)} - 1 \right) \nabla_\theta \log \pi_\theta(o | q) \right]. \quad (51)$$

Expanding $f(q, o)$ and $Z_\tau(\theta; q)$ gives exactly (18)–(19).

Finally, for the Monte Carlo form, let $\{o_i\}_{i=1}^G$ be i.i.d. samples from $\pi_\theta(\cdot | q)$ and define $f_i = f(q, o_i) = \exp(\tau \bar{d}_i) \mathbb{1}(r_i = 1)$. A plug-in estimator for $Z_\tau(\theta; q)$ is $\hat{Z} = (1/G) \sum_{j=1}^G f_j$, and for the numerator $\widehat{\nabla Z} = (1/G) \sum_{i=1}^G f_i \nabla_\theta \log \pi_\theta(o_i | q)$. Thus the ratio form in (50) yields

$$\widehat{\nabla_\theta J_\tau}(\theta; q) = \frac{1}{\tau} \cdot \frac{\widehat{\nabla Z}}{\hat{Z}} = \frac{1}{\tau} \sum_{i=1}^G \frac{f_i}{\sum_{j=1}^G f_j} \nabla_\theta \log \pi_\theta(o_i | q),$$

which corresponds to weights $\hat{w}_i = f_i / \sum_{j=1}^G f_j$, proving (20). Because $f_i = 0$ whenever $r_i = 0$, restricting to the correct set $\mathcal{P} = \{i : r_i = 1\}$ gives $\hat{w}_i \propto \exp(\tau \bar{d}_i)$ on \mathcal{P} , matching Eq. (11). \square